Available online at www.sciencedirect.com

SCIENCE DIRECT®

Biochimica et Biophysica Acta 1691 (2004) 79–90

BIOCHIMICA ET BIOPHYSICA ACTA

BBA

www.bba-direct.com

Effects of Li^+ transport and intracellular binding on Li^+/Mg^{2+} competition in bovine chromaffin cells

C.P. Fonseca[a], L.P. Montezinho[a], C. Nabais[b], A.R. Tomé[a], H. Freitas[b], C.F.G.C. Geraldes[a], M.M.C.A. Castro[a,*]

[a] *Department of Biochemistry and Centre for Neuroscience of Coimbra, University of Coimbra, P.O. Box 3126, 3001-401 Coimbra, Portugal*

[b] *Department of Botanics, University of Coimbra, Coimbra, Portugal*

Received 21 October 2003; received in revised form 16 December 2003; accepted 17 December 2003

Abstract

Li^+ transport, intracellular immobilisation and Li^+/Mg^{2+} competition were studied in Li^+-loaded bovine chromaffin cells. Li^+ influx rate constants, k_i, obtained by atomic absorption (AA) spectrophotometry, in control (without and with ouabain) and depolarising (without and with nitrendipine) conditions, showed that L-type voltage-sensitive Ca^{2+} channels have an important role in Li^+ uptake under depolarising conditions. The Li^+ influx apparent rate constant, k_{iapp}, determined under control conditions by ^7Li NMR spectroscopy with the cells immobilised and perfused, was much lower than the AA-determined value for the cells in suspension. Loading of cell suspensions with 15 mmol l^{-1} LiCl led, within 90 min, to a AA-measured total intracellular Li^+ concentration, $[Li^+]_{iT} = 11.39 \pm 0.56$ mmol (l cells)$^{-1}$, very close to the steady state value. The intracellular Li^+ T_1/T_2 ratio of ^7Li NMR relaxation times of the Li^+-loaded cells reflected a high degree of Li^+ immobilisation in bovine chromaffin cells, similar to neuroblastoma, but larger than for lymphoblastoma and erythrocyte cells. A 52% increase in the intracellular free Mg^{2+} concentration, $\Delta[Mg^{2+}]_f = 0.27 \pm 0.05$ mmol (l cells)$^{-1}$ was measured for chromaffin cells loaded with the Mg^{2+}-specific fluorescent probe furaptra, after 90-min loading with 15 mmol l^{-1} LiCl, using fluorescence spectroscopy, indicating significant displacement of Mg^{2+} by Li^+ from its intracellular binding sites. Comparison with other cell types showed that the extent of intracellular Li^+/Mg^{2+} competition at the same Li^+ loading level depends on intracellular Li^+ transport and immobilisation in a cell-specific manner, being maximal for neuroblastoma cells.

Keywords: Li^+ affinity; Intracellular Mg^{2+}; Fluorescence; NMR; Atomic absorption

1. Introduction

In spite of the successful clinical use of some lithium salts (lithium carbonate and lithium citrate) over more than 50 years as the drug of choice in the treatment of manic depression, the molecular and cellular mechanisms underlying its biochemical action are still poorly understood. These lithium salts have been shown to be mood stabilising drugs, being effective in both manic and depressive states [1,2]. Various interrelated hypotheses have been formulated to clarify the pharmacological action of Li^+. It has been reported that this ion inhibits several cellular enzymes, most of them involved in signal transduction pathways, such as glycogen synthase kinase-3β [3–8], inositol monophosphatase [9–14] and adenylate cyclase [15–17]. To explain this inhibitory effect, it has been proposed that Li^+ competes with Mg^{2+} (a very well-known protein cofactor) for Mg^{2+} binding sites in several biomolecules [7,18–21], due to its similar chemical properties (Li^+ and Mg^{2+} ions have similar ionic radii and ionic potentials). We and others have studied Li^+/Mg^{2+} competition extensively in Mg^{2+}-dependent biomolecules and in cellular systems using fluorescence spectroscopy with the Mg^{2+} indicator furaptra, as well as ^7Li and ^{31}P nuclear magnetic resonance (NMR) spectroscopy [22–26]. These studies demonstrated that Li^+ competes with Mg^{2+} for phosphate groups of small phosphorylated molecules involved in second messenger systems, such as adenosine tri- and diphosphate (ATP/ADP), guanosine tri- and diphosphate (GTP/GDP) and inositol-1,4,5-triphosphate

* Corresponding author. Tel.: +351-239-853609; fax: +351-239-853607.

E-mail address: gcastro@ci.uc.pt (M.M.C.A. Castro).

0167-4889/$ - see front matter © 2004 Elsevier B.V. All rights reserved.
doi:10.1016/j.bbamcr.2003.12.005

(IP_3) [22,23,27], for guanine-nucleotide binding G proteins [28] and for phosphate groups of erythrocyte membrane phospholipids [29]. Moreover, Li^+/Mg^{2+} competition also occurs in Mg^{2+} intracellular binding sites in Li^+-loaded human erythrocytes [22,26] and human SH-SY5Y neuroblastoma cells [21,24]. The ^7Li NMR spectroscopic technique also proved to be useful to investigate Li^+ transport [30] and intracellular binding [31].

Chromaffin cells are excitable endocrine cells, which are good neuronal models [32] and whose neurotransmitter release is enhanced by Li^+ loading [33–35]. In the present work, atomic absorption (AA) spectrophotometry and ^7Li NMR spectroscopy were used to examine Li^+ uptake and intracellular Li^+ binding in bovine chromaffin cells, whereas fluorescence spectroscopy, using the Mg^{2+}-specific fluorescent probe furaptra allowed us to quantify intracellular competition between Li^+ and Mg^{2+} ions. The NMR and fluorescence results from this work were compared with preliminary data already obtained with chromaffin cells under different experimental conditions [25] and with other cell types [24,30,31,36]. The present NMR studies were carried out with the cells immobilised and under continuous perfusion, while the fluorescence studies were performed while frequently replacing the incubation medium. These conditions constitute a major improvement relative to previous work [25], since they ensure the viability of the cells for a longer period of time and minimise artefacts resulting from the leakage of the fluorescent probe from the cell. These studies, besides investigating the membrane transport pathways involved in Li^+ uptake by chromaffin cells, under resting and excitable conditions, also aim at establishing the generality of the ionic competition model described above, contributing to the understanding of the pharmacological action of Li^+ at the molecular level.

2. Materials and methods

2.1. Materials

Furaptra (2-[2-(5-carboxy)oxazole]-5-hydroxy-6-aminobenzofuran-*N*,*N*,*O*-triacetic acid) (salt form), furaptra-AM (cell permeant acetoxymethyl (AM) ester form) and Pluronic® F-127 were obtained from Molecular Probes (Leiden, The Netherlands). Collagenase (type B), Percoll and fetal calf serum (FCS) were purchased, respectively, from Boehringer Mannheim (Mannheim, Germany), Pharmacia Biotech AB (Uppsala, Sweden) and Seromed Biochrom (Berlin, Germany). The shift reagent Na_3H_2Tm(DOTP) 3NaCl, Dulbecco's modified Eagle's medium/Ham's nutrient mixture F-12 (DMEM/F-12, 1:1 mixture), Urografin® and tetrodotoxin (TTX) were obtained from Macrocyclics (Richardson, Texas, USA), GibcoBRL Life Technologies (Gaithersburg, MD, USA), Schering AG (Berlin, Germany) and Tocris (Ballwin, MO, USA), respectively. KCl, $CaCl_2$ and $MgCl_2$ were purchased from Merck (Darmstadt, Germany). Bovine serum albumin (BSA), trypan blue, neutral red, antibiotic-antimycotic, *N*-2-hydroxyethylpiperazine-*N*′-2-ethanesulfonic acid (HEPES), ethylene glycol-bis(2-aminoethylether)-*N*,*N*,*N*′,*N*′-tetraacetic acid (EGTA), poly-L-lysine, $NaHCO_3$, LiCl, NaCl, glucose, $LaCl_3$, choline-Cl, ouabain, nitrendipine, and low-gelling temperature agarose were purchased from Sigma Company (St. Louis, MO, USA).

2.2. Isolation and culture of bovine chromaffin cells

Chromaffin cells were isolated from bovine adrenal medulla by collagenase B digestion and purified on a continuous Percoll density gradient, as described before [37]. Cell viability was checked for each preparation by the Trypan Blue exclusion method [38]. The purity of cell preparations was analysed by the Neutral Red dye test [39], which showed that 65–80% of the cells in the preparation were chromaffin cells. The cells were cultured in a 1:1 mixture DMEM/F-12 (1.56%) medium with 15 mmol l^{-1} HEPES, 26 mmol l^{-1} $NaHCO_3$, and supplemented with 5% of heat-inactivated FCS, 100 units ml^{-1} of penicillin, 100 μg ml^{-1} of streptomycin and 0.25 μg ml^{-1} of amphotericin B, at 37 °C, in a humidified CO_2 (5%) and air (95%) atmosphere.

For the AA and NMR experiments, the cells were cultured up to a density of 1×10^6 cells ml^{-1} in 100 mm Petri dishes, and maintained in culture for 3 days before the assays. For the fluorescence experiments, the cell preparation was further purified using an Urografin gradient [40], and the cells were plated at a density of 0.8×10^6 cells cm^{-2} on square (1 cm^2) coverslips previously coated with poly-L-lysine. The cells were maintained in culture for 2 days before the experiments.

2.3. Characterisation of Li^+ influx pathways in bovine chromaffin cells by AA spectrophotometry

Several aliquots of 3×10^6 bovine chromaffin cells, maintained in suspension, were incubated at 37 °C in a culture medium containing 15 mmol l^{-1} LiCl. The experiments were performed in the absence (control experiments) and in the continuous presence of ouabain, an inhibitor of the (Na^+, K^+)-ATPase (50 μmol l^{-1}, 5 min of preincubation in a LiCl-free culture medium). Other influx experiments were performed under continuous depolarising conditions (in culture medium containing 45 mmol l^{-1} KCl and 15 mmol l^{-1} LiCl) in the absence (control-KCl) and in the presence of nitrendipine, a specific blocker of the L-type voltage-sensitive Ca^{2+} channels (10 μmol l^{-1}; 5 min of preincubation in a LiCl-free culture medium) during the time course of the experiment. The cells were collected at different time points (1, 10, 20, 30, 45, 60, 90, and 150 min) and the extracellular Li^+ was removed by washing the cells with an ice-cold choline Krebs medium (in mmol l^{-1}:

choline-Cl 140, KCl 5, $CaCl_2$ 2, $MgCl_2$ 1, glucose 10, HEPES 20, pH 7.35). The use of this medium prevents Li^+ efflux as described before [30]. The cells were then lysed in 500 μl of deionised water, and dissolved in 500 μl of perchloric acid (0.15 mol l^{-1} final concentration). The lysates were then analysed by AA spectrophotometry using a Perkin Elmer AAnalyst 100 apparatus equipped with a flame source. For each experiment, the cytocrits (percentage of cell volume in the sample) were measured using an International microcapillar centrifuge, Model MB (IEC), and estimated to be approximately 2–3%. The dilution of the analysed solutions was taken into account in the determination of the total intracellular Li^+ concentrations, $[Li^+]_{iT}$.

Li^+ concentrations were obtained from the AA spectrophotometer analysis using a calibration curve (Li absorption vs. Li^+ concentration). This calibration curve was obtained by registering the Li absorption intensity of three standard solutions, with three different LiCl concentrations: 0.75, 1.5 and 3 mg l^{-1}.

The kinetics of Li^+ influx in these cells was analysed using the equation:

$$([Li^+]_{iT})_t = ([Li^+]_{iT})_\infty [1 - \exp(-k_i t)] \quad (1)$$

where k_i is the rate constant for Li^+ influx, $([Li^+]_{iT})_t$ and $([Li^+]_{iT})_\infty$ are the total intracellular Li^+ concentrations at the different time points (t) and when a steady state has been reached, respectively. The kinetic parameters were obtained by nonlinear least squares fitting of the experimental data to a monoexponential function using the Origin™ 5.0 program (Microcal™ Software, Inc, USA). A Student's unpaired two-tailed t-test was used to ascertain which differences between rate constants were significant. A value of $P < 0.05$ was considered significant.

2.4. Li^+ influx studies in bovine chromaffin cells by ^7Li NMR spectroscopy

Bovine chromaffin cells were collected, after 3 days in culture, and centrifuged at 115 × g during 8 min at 25 °C (Sigma 3K10). The pellet was resuspended in culture medium up to a volume of 500 μl. The cells were immobilised in agarose gel threads, placed in a 10 mm NMR tube and perfused with oxygenated culture medium (5% CO_2/95% O_2), at 37 °C, supplemented with 7 mmol l^{-1} of the shift reagent $[Tm(HDOTP)]^{4-}$ (thulium(III)-1,4,7,10-tetrazacyclododecane-N,N',N'',N'''-tetramethylenephosphonate) [25,30] and later with 15 mmol l^{-1} LiCl, pH 7.35. The cell immobilisation was performed by mixing the 500 μl of cell suspension (50–75 × 10^6 cells) with 500 μl of Krebs medium (in mmol l^{-1}: NaCl 140, KCl 5, $CaCl_2$ 2, $MgCl_2$ 1, glucose 10, HEPES 20, pH 7.35) containing 2% of low-gelling temperature agarose, in a 1:1 proportion (final agarose concentration of 1%), at 37 °C. The threads were formed by passing this cell mixture through a Teflon tubing with 0.5-mm internal diameter, partially submersed in ice. Once it had passed through the iced portion of the tubing, the mixture solidified and threads with 0.5-mm diameter were formed into the 10 mm NMR tube. The immobilised cells were continuously perfused at approximately 1 ml min^{-1} with culture medium containing 7 mmol l^{-1} $[Tm(HDOTP)]^{4-}$, pH 7.35. LiCl was added to the perfusate medium to have a final concentration of 15 mmol l^{-1} and the influx experiment was considered to start (time zero) when the amount of extracellular $^7Li^+$ in the NMR tube became constant as monitored by consecutive acquisitions of ^7Li NMR spectra.

The ^7Li NMR spectra were acquired at 194.3 MHz and 37 ± 0.1 °C, during 3 h. For these experiments, the following parameters were used: 64 transients (total accumulation time of 11 min for each spectrum), spectral width of 5600 Hz, pulse width of 15 μs, interpulse delay of 10 s and acquisition time of 0.360 s. The signal-to-noise ratio was enhanced by exponential multiplication with a line broadening of 30 Hz.

The kinetics of Li^+ influx in these cells was analysed using the equation:

$$[(A_i)_t/(A_i + A_e)_t] = [(A_i)_\infty/(A_i + A_e)_\infty][1 - \exp(-k_{iapp}\ t)] \quad (2)$$

where k_{iapp} is the apparent rate constant for Li^+ influx, $(A_i)_t$, $(A_e)_t$ and $(A_i)_\infty$, $(A_e)_\infty$ are the areas of the intracellular and extracellular $^7Li^+$ NMR signals at the different times (t) and when the intracellular Li^+ concentration has reached a steady state, respectively. The total area of intra- and extracellular $^7Li^+$ NMR signals, $(A_i + A_e)$, is constant with time. The k_{iapp} values were obtained by nonlinear least squares fitting of the experimental data to a monoexponential function using the Origin™ 5.0 program (Microcal™ Software).

2.5. Li^+ immobilisation within bovine chromaffin cells

The study of the degree of Li^+ immobilisation within bovine chromaffin cells was carried out by determination of the T_1 (longitudinal or spin-lattice) and T_2 (transversal or spin–spin) relaxation times of the intracellular $^7Li^+$ NMR resonance when the steady state intracellular Li^+ concentration was reached during Li^+-loading incubations. Relaxation times, T_1 and T_2, were measured using the inversion-recovery and Carr–Purcell–Meiboom–Gill (CPMG) pulse sequences, respectively, after Li^+ influx experiments monitored by ^7Li NMR spectroscopy. The intracellular $^7Li^+$ NMR T_1/T_2 ratio was used as a qualitative measure of Li^+ immobilisation inside the cells [31].

2.6. Cell viability in agarose-embedded bovine chromaffin cells

To monitor cell viability during the time course of ^7Li NMR studies, proton decoupled ^{31}P NMR spectra were

acquired at 202.3 MHz and 37 ± 0.1 °C, before Li^+ influx experiments and after T_1 and T_2 relaxation times determinations. The acquisition parameters were as follows: 1200 transients (total accumulation time of 30 min), spectral width of 14998 Hz, a 60° pulse (pulse width of 18 μs), interpulse delay of 0.55 s and acquisition time of 0.996 s. The signal-to-noise ratio was enhanced by exponential multiplication with a line broadening of 30 Hz. H_3PO_4 85% was used as an external reference (0 ppm). All the NMR experiments were performed on a Varian Unity-500 NMR spectrometer equipped with a multinuclear 10-mm broadband probe and a temperature control unit.

2.7. Li^+/Mg^{2+} competition studies by fluorescence spectroscopy

The fluorescence experiments were performed on a SPEX FluoroMax Fluorimeter, at 30 °C, using furaptra, a Mg^{2+}-specific dye at physiological pH value and Ca^{2+} levels [41,42]. The binding of this indicator to Mg^{2+} results in a blue shift in the excitation spectrum from 370 to 335 nm with increasing amounts of Mg^{2+}. The chemical properties of this probe have already been described in the literature [43].

Bovine chromaffin cells adherent to 1 cm^2 square poly-L-lysine coated coverslips (0.8×10^6 cells cm^{-2}) were washed with Krebs medium containing 1% of BSA and loaded for 45 min, in an humidified CO_2 (5%) and air (95%) atmosphere, at 37 °C, in this medium also containing 5 μM of the cell-permeant acetoxymethyl ester of furaptra (furaptra-AM) and 0.1% Pluronic® F-127, previously sonicated for 3 min. After loading the cells with the fluorescent probe, they were incubated for an additional period of 20 min in Krebs medium containing 1% BSA and then washed with a Krebs medium containing 0.2% BSA.

The coverslips with the cells (previously washed with Krebs medium) were then attached to plastic holders and placed in a fluorescence cuvette containing 1.5 ml of Krebs medium. The emission wavelength was fixed to 500 nm, and the excitation wavelength changed between 300 and 400 nm (5 nm emission and excitation slits). In the Li^+ experiment, a modified Krebs medium containing 15 mmol l^{-1} LiCl was used (NaCl was partially replaced in order to maintain the osmolarity of the medium). During all the experiments (in the absence—control—and in the presence of Li^+), the medium was changed every 15 min, along 135 min (before changing the medium to the Li^+-modified Krebs medium, the fluorescence intensity of the probe was monitored for 45 min; after that, the fluorescence was monitored during the time course of the Li^+ experiment for an additional period of 90 min), to remove any fluorescent probe that might have been released from the cells to the incubation medium. This procedure prevents the binding of the probe to the extracellular Mg^{2+}, which would contribute to an overestimated value of the intracellular free Mg^{2+} concentration, $[Mg^{2+}]_f$, and also ensures a higher cellular viability. The fluorescence intensity ratio at 335 and 370 nm, $R=(F_{335}/F_{370})$, was measured every 15 min, immediately after replacing the medium, and the $[Mg^{2+}]_f$ was determined by direct application of Eq. (3), which corrects for Li^+ binding to furaptra [23]:

$$[Mg^{2+}]_f = K_d S_{min}(R - R_{min})/S_{max}(R_{max} - R) + K_d S'_{max}(R - R'_{max})[Li^+]_{if}/K'_d\, S_{max}(R_{max} - R) \quad (3)$$

where R_{min}, R_{max} and R'_{max} are the ratios of the fluorescence intensities at 335 and 370 nm observed for the biological sample in the absence of metal ions and in the presence of saturating amounts of Mg^{2+} or Li^+, respectively; S_{min}, S_{max} and S'_{max} are the fluorescence intensities at 370 nm, respectively, in the absence of metal ions and in the presence of saturating amounts of Mg^{2+} or Li^+; K_d and K'_d are the dissociation constants of the furaptra-Mg^{2+} and furaptra-Li^+ complexes, respectively. The K_d and K_d' values were previously calculated to be 1.5 mmol l^{-1} [43] and 237 mmol l^{-1} at 37 °C [23], respectively. In this equation, the intracellular free Li^+ concentration ($[Li^+]_{if}$) should be used, rather than the total intracellular Li^+ concentration ($[Li^+]_{iT}$) [24], as it corresponds to the Li^+ ions capable of competing with Mg^{2+} for furaptra [23].

The R_{min} and S_{min} parameters were determined in a Mg^{2+}-free and Ca^{2+}-free solution (in mmol l^{-1}: KCl 120, NaCl 20, HEPES 10, EGTA 1, pH 7.35) containing 2 μmol l^{-1} of furaptra (salt form). To calculate S'_{max} 3.5 mol l^{-1} LiCl was added to the previous solution also in the presence of the same concentration of the dye. The R_{max} and S_{max} parameters were determined by adding the salt form of furaptra (2 μmol l^{-1}) to a Mg^{2+}-saturated solution (in mmol l^{-1}: $MgCl_2$ 70, KCl 15, NaCl 20, HEPES 10, pH 7.35).

3. Results

3.1. Li^+ influx experiments by atomic absorption spectrophotometry

AA spectrophotometry was used to investigate the membrane transport pathways involved in the uptake of Li^+ by chromaffin cells during loading experiments. Fig. 1 compares the dependence of the total intracellular Li^+ concentration on incubation time in the control situation and in the presence of the (Na^+, K^+)-ATPase inhibitor ouabain. The kinetics of Li^+ influx under depolarising conditions (45 mmol l^{-1} KCl) in the absence and in the presence of nitrendipine, a specific blocker of the L-type voltage-sensitive Ca^{2+} channels, is also shown. All these experiments were carried out at constant cell number (cytocrit of 2–3%) and total Li^+ concentration in the loading medium (15 mmol l^{-1}). In all cases, the intracellular Li^+ concentration

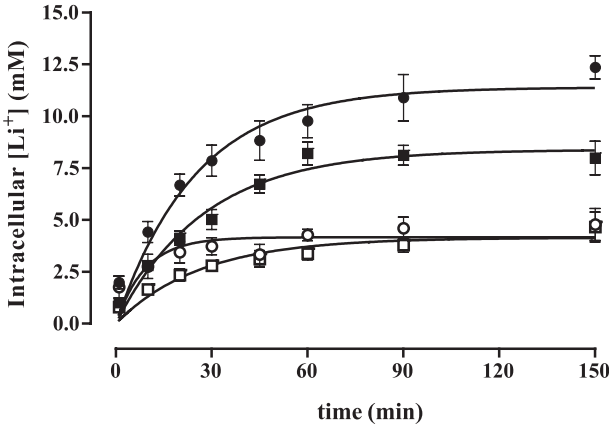

Fig. 1. Plots of $[Li^+]_i$ (determined by AA spectrophotometry) vs. loading time during Li^+ influx experiments on bovine chromaffin cells in suspension subject to loading with 15 mmol l^{-1} LiCl. Data are for control (●), in the presence of ouabain (■), in the presence of KCl (○), and in the presence of KCl and nitrendipine (□). The lines correspond to the best exponential fits of the data to Eq. (1) (see Materials and methods).

increases up to 60–90 min and then reaches a steady state, except for the experiment done under depolarising conditions without nitrendipine, where the steady state is reached earlier, at 30 min.

Li^+ influx rate constant (k_i) values, obtained from the curves presented in Fig. 1 using Eq. (1), are summarised in Table 1. The k_i value in the presence of 50 μmol l^{-1} ouabain (0.036 ± 0.005 min^{-1}, $n=7$) does not differ significantly ($P=0.69$) from the control k_i value (0.040 ± 0.006 min^{-1}, $n=14$). However, a significant increase in k_i value is observed (0.110 ± 0.038 min^{-1}, $n=5$, $P=0.01$) when the cells are depolarised with 45 mmol l^{-1} KCl, an effect that is completely suppressed in the presence of 10 μmol l^{-1} nitrendipine (0.038 ± 0.007 min^{-1}, $n=8$, $P=0.04$, Fig. 1 and Table 1).

The steady state values of intracellular Li^+ concentration, $[Li^+]_{iT}$, obtained by AA spectrophotometry, for bovine chromaffin cells, in the absence (control) and in the presence of inhibitors are also shown in Table 1. Under the control situation, the $[Li^+]_{iT}$ was determined to be 11.39 ± 0.56 mmol (l cells)$^{-1}$ ($n=14$), significantly higher than the values obtained in the presence of ouabain ($[Li^+]_{iT}=8.38 \pm 0.38$ mmol (l cells)$^{-1}$, $n=7$, $P=0.00$) and under direct depolarisation by 45 mmol l^{-1} KCl ($[Li^+]_{iT}=4.16 \pm 0.27$ mmol (l cells)$^{-1}$, $n=5$, $P=0.00$) (Fig. 1 and Table 1). The $[Li^+]_{iT}$ value observed under direct depolarising conditions (45 mmol l^{-1} KCl) in the presence of nitrendipine is not significantly different from the value in its absence ($[Li^+]_{iT}=4.14 \pm 0.28$ mmol (l cells)$^{-1}$, $n=8$, $P=0.96$, Fig. 1 and Table 1).

Table 1
Li^+ influx rate constants[a,b] and steady state intracellular Li^+ concentrations[c] for bovine chromaffin cells in the absence (control) and in the presence of inhibitors, obtained by AA and by NMR

Experimental conditions	k_i (min^{-1})	$[Li^+]_{iT}$[c]
Suspensions: control (AA)	0.040 ± 0.006 ($n=14$)	11.39 ± 0.56
+50 μmol l^{-1} ouabain (AA)	0.036 ± 0.005 ($n=14$)	8.38 ± 0.38
+45 mmol l^{-1} KCl (AA)	0.110 ± 0.038 ($n=5$)	4.16 ± 0.27
45 mmol l^{-1} KCl+10 μmol l^{-1} nitrendipine (AA)	0.038 ± 0.007 ($n=8$)	4.14 ± 0.28
Perfused: control (NMR)	0.012 ± 0.003 ($n=4$)[d]	–[e]

[a] The values (at 37 °C) are average ± standard error of the mean (SE) for the number (n) of trials indicated in parenthesis (refer in the text for P values).
[b] The starting Li^+ concentration in the medium was 15 mmol l^{-1}.
[c] In mmol (l cells)$^{-1}$.
[d] Apparent influx rate constant, k_{iapp}.
[e] Could not be calculated accurately.

3.2. Li^+ influx and intracellular degree of immobilisation by ^7Li NMR

^7Li NMR spectroscopy with the shift reagent $Tm(HDOTP)^{4-}$ was used to follow Li^+ cell uptake and study the degree of immobilisation of this ion inside the bovine chromaffin cells [25,30,31]. Several ^7Li NMR influx experiments were carried out using a number of cells in the range $50–75 \times 10^6$ immobilised in agarose gel threads and perfused with culture medium supplemented with 15 mmol l^{-1} LiCl and 7 mmol l^{-1} $Tm(HDOTP)^{4-}$ [25]. Fig. 2 represents the average of the results of all the influx experiments ($n=4$), showing a graphical representation of the time dependence of the percentage of intracellular ^7Li resonance area, A_i, relative to the total area of intra- and extracellular ^7Li NMR resonances, (A_i+A_e). Fitting this curve with Eq. (2) yields an apparent k_i value, k_{iapp}, because for the cells immobilised in agarose gel threads the influx rate constant has a contribution from the diffusion process of Li^+ across

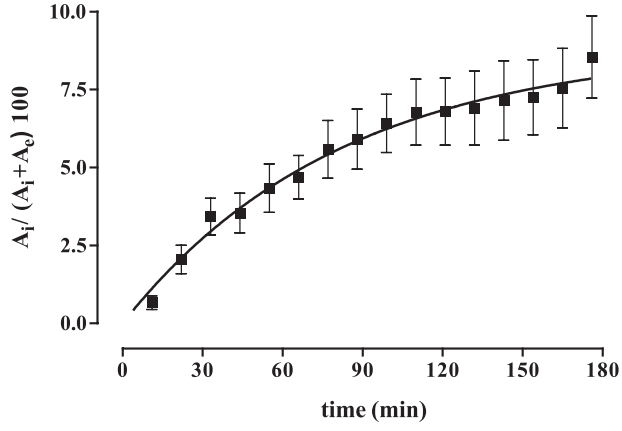

Fig. 2. Plot of the area of the intracellular $^7Li^+$ NMR signal normalized to the total area of intra- and extracellular signals, $[(A_i)/(A_i+A_e)]$, as a function of time during loading of agarose gel-embedded bovine chromaffin cells ($50–75 \times 10^6$ cells) with 15 mmol l^{-1} LiCl. The cells were perfused with the experimental medium at approximately 1 ml min^{-1}. The NMR acquisition and processing parameters used are described in Materials and methods. The experimental data was fitted using Eq. (2) (see Materials and methods). The line corresponds to the best exponential fit of the data.

Table 2
^{7}Li NMR relaxation time values[a] and T_1/T_2 ratios for intracellular Li^+ in perfused chromaffin cells and comparison with other studies on various types of cells

Sample	$[Li^+]$ (mM)[b]	T_1 (s)	T_2 (s)	T_1/T_2
Bovine chromaffin cells perfused ($n=4$)[c]	11.4	5.4 ± 1.3	0.05 ± 0.006	106 ± 28
Bovine chromaffin cells suspensions ($n=5$)[d]	1.7	6.1 ± 0.2	0.02 ± 0.002	305 ± 32
Neuroblastoma cells ($n=3$)[e]	2.9	5.1 ± 0.8	0.05 ± 0.02	102[f]
Lymphoblastoma cells ($n=3$)[g]	3.1	2.6 ± 0.4	0.06 ± 0.01	43 ± 4
Human RBCs ($n=3$)[h]	3.5	6.5 ± 0.2	0.46 ± 0.01	14[f]
Viscosity adjusted LiCl solution[h,i]	4.0	3.9 ± 0.4	3.6 ± 0.6	1.1 ± 0.2

[a] Each T_1 and T_2 value is an average ± standard error of the mean (SE) for the number (n) of trials indicated in parenthesis.
[b] For the cell samples, this is the steady state intracellular Li^+ concentration of Li^+-loaded cells, $[Li^+]_i$, expressed as mmol (l cells)$^{-1}$, with errors less than 10%.
[c] This work.
[d] Data from Ref. [25].
[e] Data from Ref. [30].
[f] Errors are less than 10%.
[g] Data from Ref. [36].
[h] Data from Ref. [31].
[i] Sample viscosity was adjusted to 5 centipoise (cP) with glycerol.

the gel before reaching the cell membrane [44]. The average value obtained for k_{iapp} is 0.012 ± 0.003 min^{-1}.

Three hours after the beginning of the $^{7}Li^+$ influx NMR experiments, when the steady state intracellular Li^+ concentration was reached (Fig. 2), the Li^+ degree of immobilisation inside the chromaffin cells was investigated using ^{7}Li NMR relaxation measurements by determining intracellular $^{7}Li^+$ T_1 and T_2 values and the respective T_1/T_2 ratio, which is a sensitive measure of Li^+ immobilisation [25,30,31,36]. Table 2 compares the results obtained in this work with those from previous studies in other types of cells [24,25,30,31,36].

3.3. ^{31}P NMR spectra of agarose-embedded bovine chromaffin cells

Cell viability of the agarose-embedded bovine chromaffin cells was monitored, in the experimental conditions of the perfusion experiments, by obtaining ^{31}P NMR spectra during the time course of the ^{7}Li NMR experiments. Fig. 3 shows a proton-decoupled ^{31}P NMR spectrum obtained after a sequence of Li^+ influx and intracellular ^{7}Li T_1 and T_2 relaxation measurements (a total of 7 h 30 min of perfusion). The assignments of the ^{31}P spectral resonances of phosphorylated cell metabolites, such as ATP, phosphomonoesters (PME), sugar phosphates (sugar-P) and inorganic phosphate (P_i), were taken from data previously published on immobilised and perfused bovine chromaffin cells [45]. This spectrum shows the compartmentation of some of these metabolites, namely of ATP, in the cytosol and inside the granules. The ^{31}P NMR signal of cytosolic P_α-ATP is not observable, as it is part of the composite peak at −10.8 ppm with the resonance from intragranular P_α-ATP, as well as from the vesicular P_α-ADP and the bisphosphate moiety of NAD^+ and NADH [45].

3.4. Li^+/Mg^{2+} competition studies by fluorescence spectroscopy

Li^+/Mg^{2+} competition studies in bovine chromaffin cells were carried out by fluorescence spectroscopy using the Mg^{2+} fluorescent probe furaptra. According to established

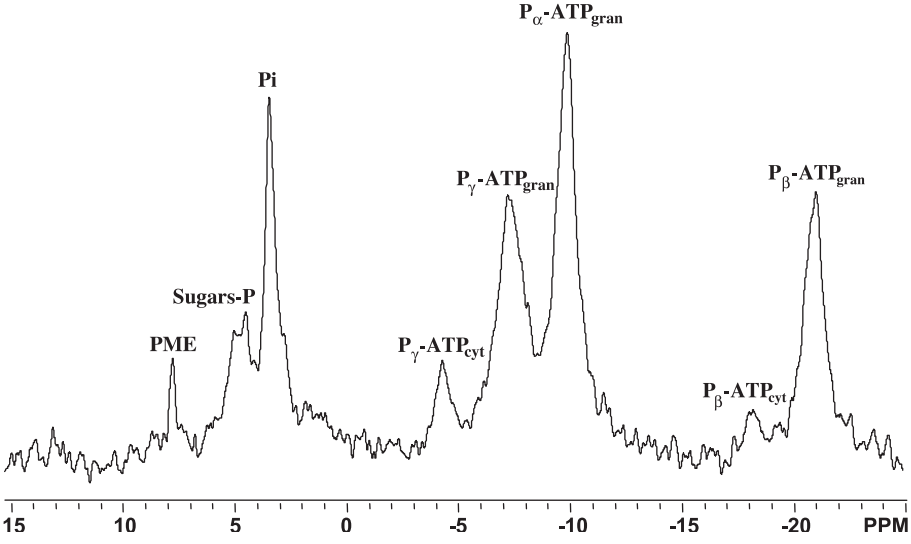

Fig. 3. ^{1}H-decoupled ^{31}P NMR spectrum of Li^+-loaded agarose gel-embedded bovine chromaffin cells (50−75 × 10^{6} cells), after 7 h 30 min perfusion. See Materials and methods for NMR acquisition and processing parameters. PME: phosphomonoesters; Sugar-P: sugars phosphate groups; P_i: inorganic phosphate; P_α-, P_β- and P_γ-ATP_{cyt}: α, β and γ phosphate groups, respectively, of cytosolic ATP; P_α-, P_β- and P_γ-ATP_{gran}: α, β and γ phosphate groups of granular ATP, respectively.

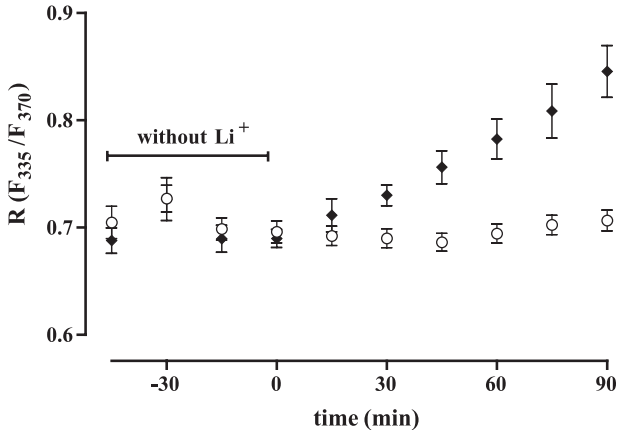

Fig. 4. Time dependence of fluorescence intensity ratio $R=F_{335}/F_{370}$ in bovine chromaffin cells previously loaded with the Mg^{2+} fluorescent probe furaptra, under control Li^+-free conditions (▽) and when the cells were incubated for 90 min with 15 mmol l^{-1} LiCl (◆).

data [23–25], an increase in the ratio of fluorescence intensities at 335 nm and 370 nm, $R=F_{335}/F_{370}$, during Li^+ cell loading is indicative of Mg^{2+} binding to furaptra (salt form) inside the cells, which is a consequence of the displacement of Mg^{2+} by Li^+ from its binding sites. The R values are converted into intracellular free Mg^{2+} concentration, $[Mg^{2+}]_f$, using Eq. (3). The Li^+/Mg^{2+} competition depends on the type of cells and on the intracellular free Li^+ concentration, which, in turn, is dependent on the extracellular Li^+ concentration (data not shown). Fig. 4 shows a graphical representation of the time dependence of the R values for a control situation (in the absence of Li^+) and for a 90 min Li^+-loading experiment using a total Li^+ concentration in the medium of 15 mmol l^{-1}. In the former experiment, the basal R value, which corresponds to $[Mg^{2+}]_f=0.54\pm0.01$ mmol (l cells)$^{-1}$ ($n=12$) ($[Li^+]_{if}=0$), was maintained over time for 135 min. In the latter experiment, while at the time zero of Li^+ loading $[Mg^{2+}]_f$ was not significantly different from the previous one ($[Mg^{2+}]_f=0.52\pm0.02$ mmol (l cells)$^{-1}$ ($n=6$), $P=0.21$), $[Mg^{2+}]_f$ increased very significantly (by 52%) during the 90 min of the Li^+ loading process to a value of 0.79 ± 0.05 mmol (l cells)$^{-1}$ (see Discussion).

4. Discussion

Li^+ accumulates inside the cells via different mechanisms, such as passive diffusion, voltage-dependent Na^+ channels and by replacing Na^+ in counter-transport mechanisms, while it is not extruded via the (Na^+, K^+)-ATPase [30, 46]. Initially, only influx occurs, but as intracellular Li^+ builds up, Li^+ efflux also takes place until a steady state intracellular Li^+ concentration, determined by the membrane potential, is reached. In the present study of the Li^+ uptake by chromaffin cells in suspension, the k_i value for the control (0.040 ± 0.006 min^{-1}, $n=14$) obtained by AA spectrophotometry is similar to the value reported for bovine chromaffin cells in suspension ($k_i=0.040\pm0.003$ min^{-1}, $n=4$) obtained by ^{7}Li NMR [25]. However, as expected from the slow Li^+ diffusion across the gel before reaching the cells, these two values are significantly higher than the one obtained by ^{7}Li NMR for chromaffin cells immobilised in agarose gel threads ($k_{iapp}=0.012\pm0.003$ min^{-1}, $n=4$; $P=0.02$ and $P=0.00$ when compared to the k_i value obtained for chromaffin cells in suspension using both AA spectrophotometry and ^{7}Li NMR spectroscopy [25], respectively).

The kinetics of Li^+ influx, as shown by AA spectrophotometry, is not affected in the presence of ouabain, which is in agreement with the noninvolvement of (Na^+, K^+)-ATPase in Li^+ uptake by chromaffin cells, under resting conditions. However, when the cells are depolarised with 45 mmol l^{-1} KCl, a significant increase in k_i value is observed, an effect that is completely suppressed in the presence of 10 μmol l^{-1} nitrendipine. This is a clear indication that, under increased cellular excitability conditions, a new contribution to Li^+ influx appears, which results from activation of L-type voltage-sensitive Ca^{2+} channels. Cell depolarisation leads to a massive Ca^{2+} entry and to a large increase of intracellular Ca^{2+} concentration, which increases the activity of the Na^+/Ca^{2+} exchanger, known to be a high-capacity, low-affinity mechanism of Ca^{2+} efflux in chromaffin cells [47,48]. It is well known that Li^+ can replace Na^+ in the Ca^{2+} influx via the Na^+/Ca^{2+} exchanger pathway in Li^+-loaded chromaffin cells [33,35] and in rat skeletal muscle cells [49], where Ca^{2+} influx is counterbalanced by Li^+ efflux. In the present case of Li^+ loading of the chromaffin cells, we propose that the Na^+/Ca^{2+} exchanger uses the external Na^+ and Li^+ to remove intracellular Ca^{2+}. Blocking of the L-type voltage-sensitive Ca^{2+} channels by nitrendipine prevents the Ca^{2+} entry through these channels when cell depolarisation occurs and therefore depresses the activity of the Na^+/Ca^{2+} exchanger, suppressing this new Li^+ entry pathway.

Li^+ transport pathways have been shown to be highly cell-type specific [30,36,46,50]. (Na^+, K^+)-ATPase provides a major Li^+ influx pathway in lymphoblastoma cells [36], but it is not active in red blood cells (RBCs) [46] and in chromaffin cells, as shown in this work. The 4,4′-diisothiocyna-2,2′-disulfonic stilbene (DIDS)-sensitive anion exchange pathway is a major contributor to Li^+ influx in RBCs [46], but not in neuroblastoma or lymphoblastoma cells [30,36]. In human neuroblastoma SH-SY5Y cells and other excitable cells, it has been shown that voltage-sensitive Na^+ channels contribute to Li^+ influx [30,46], but not in lymphoblastoma cells [36,51]. In bovine chromaffin cells, besides the known Li^+ influx pathway using voltage-sensitive Na^+ channels [33,52], we propose here a Ca^{2+}-dependent Li^+ influx pathway in depolarising conditions, where Li^+ replaces Na^+ in the Na^+/Ca^{2+} counter-transport.

In the absence of active transport pathways for Li^+ influx in chromaffin cells, the steady state values of

intracellular Li^+ concentration obtained, $[Li]_{iT}$, which reflect the capacity of the cells to accumulate Li^+, are controlled by the plasma membrane potential, which has a resting value of −55 mV [53]. When depolarisation occurs, the membrane potential becomes less negative, and the total amount of positively charged ions (such as Li^+) that can be accumulated by the cells is lowered, when compared to the control situation, due to charge effects (see Fig. 1 and Table 1). This dependence is demonstrated by the observation that the amount of Li^+ accumulated by the cells is significantly lowered when they are directly depolarised by 45 mmol l^{-1} KCl. The $[Li^+]_{iT}$ values observed under direct depolarising conditions in the presence and in the absence of nitrendipine are not significantly different, as expected, since in these conditions the membrane potential is kept constant by the high extracellular K^+ concentrations, even if nitrendipine affects the Li^+ uptake kinetics. The observation that ouabain, which has no effect on the kinetics of Li^+ uptake, lowers the steady state $[Li^+]_{iT}$ also shows its depolarising effect on these cells [54].

The present results also show that, under the same cell loading conditions (15 mmol l^{-1} LiCl), the steady state $[Li^+]_{iT}$ value reached for the chromaffin cells in resting, nondepolarised control conditions is much higher than that reported for veratridine nonstimulated human neuroblastoma SH-SY5Y cells (2.9 mmol (l cells)$^{-1}$ [30], despite having similar resting membrane potentials, −55 mV for chromaffin cells [53] and −53 mV for neuroblastoma SH-SY5Y cells [55]. Lymphoblastoma, neuroblastoma and RBCs cells have been found to reach $[Li^+]_{iT}$ values in the range of 14.5, 11.5 and 6.0 mmol (l cells)$^{-1}$, respectively, after 60 min loading with 50 mmol l^{-1} LiCl [36]. In this case, the relative accumulation of Li^+ by the cells partially follows the trend of their membrane potentials, which are more negative for the former two types of cells (range of −50 to −90 mV) [51,55] than for RBCs (−10 mV) [46]. Thus, variations in Li^+ transport pathways cause further Li^+ accumulation differences in the various cell types studied.

While it is easy to follow the kinetics of Li^+ uptake by the perfused chromaffin cells through the time dependence of the area (A_i) of the intracellular ^7Li NMR resonance (Fig. 2), intracellular Li^+ concentrations, $[Li^+]_i$, could not be calculated from this area because the cell volume cannot be determined by the ^7Li NMR method [30]. The fitting procedure of the data of Fig. 2 using Eq. (2) gave values of intracellular-to-total signal area ratios $[A_i/(A_i+A_e)]$ of $(5.91 \pm 0.96) \times 10^{-2}$ ($n=4$) at 90 min and of $(8.89 \pm 1.09) \times 10^{-2}$ ($n=4$) at steady state. A rough estimate of the cell volume was made, based on the average cell diameter [56] and the average number of cells (65.7×10^6, $n=4$) used in the samples. Assuming that the cells are uniformly dispersed in the gel, this cell volume estimate was used together with an assumed total sample volume of 1 ml, a total Li^+ concentration of 15 mmol l^{-1}, and the experimental $[A_i/(A_i+A_e)]$ ratios to obtain rough estimates of the intracellular Li^+ concentrations at 90 min and at steady state. These estimates are 20–40% lower than the corresponding intracellular Li^+ concentrations determined by AA spectrophotometry, $[Li^+]_{iT}$. One possible reason for this discrepancy between estimates of intracellular Li^+ concentrations measured by the two techniques is that while the AA-derived values correspond to the total intracellular concentrations, including granular and cytosolic, free and bound Li^+, the weakly quadrupolar $^7Li^+$ nuclei may be partially NMR invisible when bound in the highly viscous granular compartment.

It must be pointed out that the (AA- and NMR-derived) intracellular Li^+ concentrations expressed per liter of cells are not directly comparable with concentrations expressed per liter of water (e.g., extracellular concentrations). The later ones are considerably higher because the ratio of volume of intracellular water accessible to Li^+ ions to cell volume is $\alpha<1$, owing to the presence of membranes, organelles and cytosolic proteins. For example, if granular Li^+ is not NMR observable (the granular compartment accounts for about 10% of the cellular volume), as the cytosolic volume is about 50% of the extragranular cell volume [57], an $\alpha=0.45$ value would give $[Li^+]_i$ mmol l^{-1} values more than twice the mmol (l cells)$^{-1}$ values.

The T_1/T_2 ratio is a sensitive measure of the rotational correlation time, τ_c, of the Li^+ ion, and hence of Li^+ immobilisation, independently of the fraction of bound Li^+ and of its binding affinity [25,30,31,36]. The T_1/T_2 ratio obtained for the bovine chromaffin cells, under the perfusion experimental conditions, is considerably lower than for the same cells in suspension [25] at similar intracellular Li^+ concentrations, indicating an increased degree of immobilisation of Li^+ in the later case. This difference could reflect some loss of viability of the cells during the NMR experiments without perfusion. The disruption of the cell membrane and the probable nonintegrity of the cytoplasm may contribute to a higher immobilisation of this ion through binding to the cytoplasmatic membrane and intracellular structures. Comparing the T_1/T_2 ratios of the various perfused cell systems at similar Li^+ loading levels (Table 2), the degree of Li^+ immobilisation is larger in bovine chromaffin cells and in SH-SY5Y human neuroblastoma cells, followed by lymphoblastoma cells and is smaller in RBCs [30,31,36]. This reflects the relative local mobility of the intracellular Li^+ binding sites of the different systems. The T_1/T_2 ratios of all these cell types are much higher than the value for an aqueous LiCl solution whose viscosity was adjusted to approximate the intracellular viscosity.

Cell viability during the time course of the ^7Li NMR experiments with the perfused cells was monitored by obtaining ^{31}P NMR spectra at the beginning and at the end of the perfusion (Fig. 3). In fact, some ^{31}P NMR parameters reflect the viability of the cells throughout the perfusion experiments. The ratio of the areas of the P_β-$ATP_{(cytosol)}$ and $P_{i(cytosol)}$ ^{31}P NMR resonances (P_β-$ATP_{(cytosol)}/P_{i(cytosol)}$), which reflects the energetic status of the cells [58], remained constant at 0.17 during the course of the NMR

experiments. The chemical shift of the P_γ-$ATP_{(granule)}$ resonance gave intragranular pH values at the beginning and at the end of the perfusion experiments of 5.47 ± 0.02 ($n=3$) and 5.52 ± 0.04 ($n=3$), respectively, which did not significantly change ($P=0.43$), as determined using the calibration curve reported in the literature [59]. These intragranular pH values, although higher than those reported in some studies (5.3) [60], are comparable to the pH reported in viable, but hypoxic, chromaffin cells (5.57 ± 0.13) [45] and of isolated chromaffin granules (5.65 ± 0.15) [61], but lower than the pH reported for oxygenated, superfused chromaffin cells cultured on polystyrene microcarrier beads (5.84 ± 0.11) [45]. Another indicator of the viability of the chromaffin cell samples, obtained through ^{31}P NMR spectra, is the observation of the cytosolic P_γ-ATP and P_β-ATP signals. When the cells are in suspension [25] or immobilised without perfusion [45], the cytosolic P_γ-ATP and P_β-ATP signals are not observed. When the cells are under good perfusion conditions, these resonances appear at approximately -4.5 and -18.4 ppm, respectively (see Fig. 3), which is indicative of cell viability during the time course of the NMR experiments. The area ratio (P_β-$ATP_{(cytosol)}$/P_β-$ATP_{(granule)}$) was reported to have a value of 0.19 in perfused chromaffin cell preparations of optimal viability [45]. After correction for the saturation factors of the cytosolic ATP signals using the experimental repetition rates and the reported ^{31}P T_1 values, this ratio was 0.17 in our samples throughout the perfusion experiments (the corresponding corrected ratio for the P_γ-ATP signals was 0.20), indicating that the viability of the perfused cells was kept throughout the experiments.

Besides being used to monitor the viability of cellular systems, ^{31}P NMR methods have been previously validated to study Li^+/Mg^{2+} competition [22], which can also be followed by fluorescence spectroscopy. In fact, the fluorescence method was found to be the most sensitive for cellular studies [23, 24]. Despite its reduced sensitivity, ^{31}P NMR has been widely used with biomolecules [22,23,29] and several cell types [24,25,62] to determine intracellular free Mg^{2+} concentrations, $[Mg^{2+}]_f$. However, this ^{31}P NMR method, which is based on the change of the measured chemical shift difference between the ^{31}P resonances of the P_α and P_β phosphate groups ($\Delta\delta_{\alpha\beta}$) of ATP due to Mg^{2+} binding [62], is not applicable to chromaffin cells due to their particular characteristics. In fact, ATP compartmentation in these cells causes the overlap of the P_α ^{31}P NMR signals of cytosolic and granular ATP (Fig. 3), preventing the use of this technique to determine $[Mg^{2+}]_f$ in the cytosol of these cells. Although $\Delta\delta_{\alpha\beta}$ can be obtained for the granular compartment, the high ionic strength and specific ATP interactions in the granule make it inappropriate to use the simple dilute aqueous model to determine $[Mg^{2+}]_f$ values accurately in this organelle [59,61,63]. However, we saw no effect of Li^+ loading on the granular $\Delta\delta_{\alpha\beta}$ value, indicating no significant Li^+/Mg^{2+} competition there.

Therefore, fluorescence spectroscopy was in this work the method of choice to study Li^+/Mg^{2+} competition in bovine chromaffin cells. The experimental conditions used here (see Materials and methods) allowed an improvement in the quality of the fluorescence data collection relative to previous data obtained by us in similar experiments with these cells in suspension [25]. Using fluorescence measurements of furaptra, the intracellular free Mg^{2+} concentration was found to increase very significantly during the 90 min of the Li^+ loading process but did not reach a steady state value. However, the accuracy of the calculation of $[Mg^{2+}]_f$ at any time point depends on the accuracy of the evaluation of the intracellular free Li^+ concentration, $[Li^+]_{if}$, in Eq. (3), which affects the negative contribution of its second term. As the Li^+ concentrations determined by AA spectrophotometry correspond to the total intracellular values, $[Li^+]_{iT}$, including granular and cytosolic, free and bound Li^+, $[Li^+]_{iT}$ values can be taken as the upper limit of $[Li^+]_{if}$, giving a lower limit to $[Mg^{2+}]_f$. However, an upper limit to $[Mg^{2+}]_f$ is more difficult to obtain, since the ^7Li NMR-derived $[Li^+]_i$ values may not accurately represent lower limit estimates of $[Li^+]_{if}$, due to the possible contribution of both free and bound NMR-visible intracellular Li^+ to the intracellular ^7Li NMR signal.

Taking these considerations into account, various estimates of $[Mg^{2+}]_f$ after 90 min of Li^+ loading were carried out. As determined by AA spectrophotometry of the cells in suspension, the intracellular Li^+ concentration reached after 90 min loading is $[Li^+]_{iT} = 10.07 \pm 0.84$ mmol (l cells)$^{-1}$ ($n=14$) (Fig. 1). Assuming that all intracellular Li^+ is free, a lower limit of $[Mg^{2+}]_f$ is obtained when using this $[Li^+]_{iT}$ value as $[Li^+]_{if}$ in Eq. (3). The calculated value for $[Mg^{2+}]_f$ at 90 min of the Li^+ loading period is 0.78 ± 0.05 mmol (l cells)$^{-1}$, corresponding to a 50% increase of intracellular free Mg^{2+} ($\Delta[Mg^{2+}]_f = 0.26 \pm 0.05$ mmol (l cells)$^{-1}$) relative to the initial value. Even if the steady state $[Li^+]_{iT}$ value is used ($[Li^+]_{iT} = 11.39 \pm 0.56$ mmol (l cells)$^{-1}$, $n=14$, Fig. 1 and Table 1), the $[Mg^{2+}]_f$ value at 90 min remains unchanged. However, taking the intracellular Li^+ concentration $[Li^+]_i$ obtained by ^7Li NMR for the immobilised, perfused cells, as a lower limit of $[Li^+]_{if}$, an upper limit value of $[Mg^{2+}]_f$ is obtained by Eq. (3). As the cells are trapped in the agarose gel, the kinetics of Li^+ loading is much slower in the immobilised cells (Fig. 2) than in suspension (Fig. 1) and, consequently, the Li^+ loading of the immobilised cells does not reach the steady state at 90 min. Thus, we should consider the ^7Li NMR derived $[Li^+]_{if}$ value for immobilised, perfused cells at steady state, $[Li^+]_{if} = 9.42 \pm 0.01$ mmol (l cells)$^{-1}$, instead of the $[Li^+]_{if}$ value at 90 min. The $[Mg^{2+}]_f$ value obtained by Eq. (3) in these conditions is 0.79 ± 0.05 mmol (l cells)$^{-1}$, corresponding to a 52% increase of intracellular free Mg^{2+}. Thus, as demonstrated here, any uncertainty in the $[Li^+]_{if}$ value to be used in Eq. (3) has a very small effect on the calculated $[Mg^{2+}]_f$ values, because the negative contribution of the second term is quite small.

The $[Mg^{2+}]_f$ increases when Li^+ enters the cells observed by fluorescence spectroscopy confirms the capacity of Li^+ to displace Mg^{2+} from its intracellular binding sites. However, it is confirmed that they are too small to be detected by the much less sensitive ^{31}P NMR spectroscopic methods [22–26]. The $[Mg^{2+}]_f$ increases estimated in the present work are much smaller than those obtained for these cells in suspension [25]. This is a result of the improved cell handling procedures used here, where errors due to the release of the probe from the cells were avoided, through periodic changes of the cell medium, which also ensures a higher cellular viability. For similar $[Li^+]_i$ values, the percent increase of $[Mg^{2+}]_f$ observed in chromaffin cells (e.g., 50% at $[Li^+]_i$ = 10.1 mmol (l cells)$^{-1}$) is very similar to the values previously described in lymphoblastoma cells (52% at $[Li^+]_i$ = 11.1 mmol (l cells)$^{-1}$), but much less than in neuroblastoma cells (158% at $[Li^+]_i$ = 15.0 mmol (l cells)$^{-1}$) and much higher than in RBCs (6% at $[Li^+]_i$ = 4.0 mmol (l cells)$^{-1}$) [24,36]. Thus, the relative extent of Li^+/Mg^{2+} competition in the different types of cells studied expressed by the percent $[Mg^{2+}]_f$ increase divided by $[Li^+]_i$ ($\%(\Delta[Mg^{2+}]_f/[Mg^{2+}]_f)/[Li^+]_i$ ratio) is: neuroblastoma ($10.5 \pm 2.0\%$) ≫ chromaffin ($4.9 \pm 0.1\%$) ≈ lymphoblastoma ($4.8 \pm 0.2\%$) ≫ RBCs ($1.5 \pm 0.9\%$) [36].

For the same total Li^+ concentration in the medium, the total Li^+ accumulation is different for the various types of cells, as it depends on the different cell membrane transport pathways, leading to the following relative order: chromaffin cells>lymphoblastoma cells>neuroblastoma cells>RBCs. The effect of the different Li^+ accumulation capacity on the percent of intracellular Li^+/Mg^{2+} competition may be compensated by increased numbers of intracellular binding sites and competition sites, as well as extent of Li^+ immobilisation, as observed in this work in chromaffin cells and also in neuroblastoma cells [36]. This may explain why the effect of Li^+ on Mg^{2+} intracellular distribution is more similar in chromaffin and lymphoblastoma cells than in neuroblastoma cells and RBCs, as a consequence of differences in Li^+ transport and immobilisation properties, as suggested by the relative percent $[Mg^{2+}]_f$ increase/$[Li^+]_i$ ratios. Thus, the extent of Li^+/Mg^{2+} competition under pharmacological conditions will be cell-type dependent.

An additional problem in the quantification of Li^+/Mg^{2+} competition in cells is the possibility of intracellular compartmentation of the probe. In fact, the fluorescent probe furaptra only gives information about Li^+/Mg^{2+} competition in the cytosol because the ester form of this probe, once inside the cell, is hydrolysed by esterases present in the cytosol [63]. In its fluorescent salt form, furaptra does not enter the granule.

This work provides further evidence for the generality of the ionic competition mechanism, whose extent depends on the particular cell types. Li^+/Mg^{2+} competition has been shown to occur at therapeutic intracellular Li^+ levels (0.6–3.1 mmol (l cells)$^{-1}$) in human neuroblastoma SH-SY5Y cells [20]. Changes in $[Mg^{2+}]_f$ of the order of 10%, observed for these cells at $[Li^+]_i$ = 0.6 mmol (l cells)$^{-1}$, are expected to have a large impact on the many biochemical and cell signalling pathways involving Mg^{2+}-dependent enzymes [36]. From the present work, and based on the experimentally observed proportional relationships in $\%(\Delta[Mg^{2+}]_f/[Mg^{2+}]_f)/[Li^+]_i$, much smaller (3%) percentage effects in $[Mg^{2+}]_f$ are to be expected in chromaffin cells at $[Li^+]_i$ = 0.6 mmol (l cells)$^{-1}$, similar to those proposed for lymphoblastoma cells (3%) and still higher than for RBCs (1.5%) [36], which possibly will have an undetectable cell impact. Thus, at therapeutic $[Li^+]_i$ levels, the extent of Li^+/Mg^{2+} competition will be cell-type specific, depending on intracellular Li^+ accumulation, binding and immobilisation.

Acknowledgements

The authors acknowledge financial support from Fundação para a Ciência e a Tecnologia (F.C.T.), Portugal (Project POCTI/1999/BCI/36160) and thank Dr. Rosa Santos for useful discussions. C.P. Fonseca and L.P. Montezinho were supported by F.C.T. grants, Praxis XXI/BD/21462/99 and SFRH/BD/3286/2000, respectively.

References

[1] N.J. Birch, in: H. Sigel (Ed.), Metal Ions in Biological Systems, vol. 14, Marcel Dekker, New York, 1982, pp. 257–313.
[2] R.H. Lenox, R.K. McNamara, R.L. Papke, H.K. Manji, Neurobiology of lithium: an update, J. Clin. Psychiatry 59 (1998) 37–47.
[3] P.S. Klein, D.A. Melton, A molecular mechanism for the effect of lithium on development, Proc. Natl. Acad. Sci. 93 (1996) 8455–8459.
[4] C.M. Hedgepeth, L.J. Conrad, J. Zhang, H.-C. Huang, V.M.Y. Lee, P.S. Klein, Activation of the Wnt signaling pathway: a molecular mechanism for lithium action, Dev. Biol. 185 (1997) 82–91.
[5] R.S. Jope, Anti-bipolar therapy: mechanism of action of lithium, Mol. Psychiatry 4 (1999) 117–128.
[6] R.S. Williams, A.J. Harwood, Lithium therapy and signal transduction, TIPS 21 (2000) 61–64.
[7] W.J. Ryves, A.J. Harwood, Lithium inhibits glycogen synthase kinase-3 by competition for magnesium, Biochem. Biophys. Res. Commun. 280 (2001) 720–725.
[8] W.J. Ryves, R. Dajani, L. Pearl, A.J. Harwood, Glycogen synthase kinase-3 inhibition by lithium and beryllium suggests the presence of two magnesium binding sites, Biochem. Biophys. Res. Commun. 290 (2002) 967–972.
[9] J.H. Allison, M.A. Stewart, Reduced brain inositol in lithium-treated rats, Nat. New Biol. 233 (1971) 267–268.
[10] L.M. Hallcher, W.R. Sherman, The effects of lithium ion and other agents on the activity of myo-inositol-1 phosphatase from bovine brain, J. Biol. Chem. 255 (1980) 10896–10901.
[11] T. Bergsma, H.S. Hiemstra, B. De Vries, J.V. Kaay, P.J.M. Haastert, *Dictyostelium discoideum* contains three inositol monophosphatase activities with different substrate specificities and sensitivities to lithium, Biochem. J. 314 (1996) 491–495.
[12] V. Saudek, P. Vincendon, Q.T. Do, A. Atkinson, V. Sklenár, P.D. Pelton, F. Piriou, A.J. Ganzhorn, ^{7}Li nuclear-magnetic-resonance study of lithium binding to myo-inositol monophosphatase, Eur. J. Biochem. 240 (1996) 288–291.

[13] J. Canales, F. Buitrago, A. Faraldo, M. Ávalos, J.C. Cameselle, Identification of rat liver glucose-3-phosphatase as an inositol monophosphatase inhibited by lithium, Arch. Biochem. Biophys. 343 (1997) 27–34.
[14] S. Patel, M. Martínez-Ripoll, T.L. Blundell, A. Albert, Structural enzymology of Li^+-sensitive/Mg^{2+}-dependent phosphatases, J. Mol. Biol. 320 (2002) 1087–1094.
[15] M.E. Newman, R.H. Belmaker, Effects of lithium in vitro and ex vivo on components of the adenylate cyclase system in membranes from the cerebral cortex of the rat, Neuropharmacology 26 (1987) 211–217.
[16] A. Mørk, A. Geisler, The effects of lithium in vitro and ex vivo on adenylate cyclase in brain are exerted by distinct mechanisms, Neuropharmacology 28 (1989) 307–311.
[17] H.K. Manji, W.Z. Potter, R.H. Lenox, Signal transduction pathways. Molecular targets for lithium's actions, Arch. Gen. Psychiatry 52 (1995) 531–543.
[18] S. Avissar, G. Schreiber, A. Danon, R.H. Belmaker, Lithium inhibits adrenergic and cholinergic increases in GTP binding in rat cortex, Nature 331 (1988) 440–442.
[19] S. Avissar, G. Schrieber, Ziskind–Somerfeld research award. The involvement of guanine nucleotide binding proteins in the pathogenesis and treatment of affective disorders, Biol. Psychiatry 31 (1992) 435–459.
[20] I.F. Gow, P.W. Flatman, D. Ellis, Lithium induced changes in intracellular free magnesium concentration in isolated rat ventricular myocytes, Mol. Cell. Biochem. 198 (1999) 129–133.
[21] B. Layden, C. Diven, N. Minadeo, F.B. Bryant, D. Mota de Freitas, Li^+/Mg^{2+} competition at therapeutic intracellular Li^+ levels in human neuroblastoma SH-SY5Y cells, Bipolar Disord. 2 (2000) 200–204.
[22] D.M. Freitas, L. Amari, C. Srinivasan, Q. Rong, R. Ramasamy, A. Abraha, C.F.G.C. Geraldes, M.K. Boyd, Competition between Li^+ and Mg^{2+} for the phosphate groups in the human erythrocyte membrane and ATP: an NMR and fluorescence study, Biochemistry 33 (1994) 4101–4110.
[23] L. Amari, B. Layden, Q. Rong, C.F.G.C. Geraldes, D.M. Freitas, Comparison of fluorescence, ^{31}P NMR and ^{7}Li NMR spectroscopic methods for investigating Li^+/Mg^{2+} competition for biomolecules, Anal. Biochem. 272 (1999) 1–7.
[24] L. Amari, B. Layden, J. Nikolakopoulos, Q. Rong, D.M. Freitas, G. Baltazar, M.M.C.A. Castro, C.F.G.C. Geraldes, Competition between Li^+ and Mg^{2+} in neuroblastoma SH-SY5Y cells: a fluorescence and ^{31}P NMR study, Biophys. J. 76 (1999) 2934–2942.
[25] C.P. Fonseca, L.P. Montezinho, G. Baltazar, B. Layden, D.M. Freitas, C.F.G.C. Geraldes, M.M.C.A. Castro, Li^+ influx and binding, and Li^+/Mg^{2+} competition in bovine chromaffin cell suspensions as studied by ^{7}Li NMR and fluorescence spectroscopy, Metal Based Drugs 7 (2000) 357–364.
[26] R. Ramasamy, D.M. Freitas, Competition between Li^+ and Mg^{2+} for ATP in human erythrocytes. A ^{31}P NMR and optical spectroscopy study, FEBS Lett. 244 (1989) 223–226.
[27] Q. Rong, D.M. Freitas, C.F.G.C. Geraldes, Competition between lithium and magnesium ions for the substrates of second messenger systems: a nuclear magnetic resonance study, Lithium 5 (1994) 147–156.
[28] N. Minadeo, B. Layden, L.V. Amari, V. Thomas, K. Radloff, C. Srinivasan, H.E. Hamm, D.M. de Freitas, Effect of Li^+ upon the Mg^{2+}-dependent activation of recombinant $G_{i\alpha1}$, Arch. Biochem. Biophys. 388 (2001) 7–12.
[29] C. Srinivasan, N. Minadeo, C.F. Geraldes, D. Mota de Freitas, Competition between Li^+ and Mg^{2+} for red blood cell membrane phospholipids: a ^{31}P, ^{7}Li, and ^{6}Li nuclear magnetic resonance study, Lipids 34 (1999) 1211–1221.
[30] J. Nikolakopoulos, C. Zachariah, D.M. Freitas, E.B. Stubbs Jr., R. Ramasamy, M.M.C.A. Castro, C.F.G.C. Geraldes, ^{7}Li nuclear magnetic resonance study for the determination of Li^+ properties in neuroblastoma SH-SY5Y cells, J. Neurochem. 71 (1998) 1676–1684.
[31] Q. Rong, M. Espanol, D.M. Freitas, C.F.G.C. Geraldes, ^{7}Li NMR relaxation study of Li^+ binding in human erythrocytes, Biochemistry 32 (1993) 13490–13498.
[32] J.M. Trifaró, The cultured chromaffin cell: a model for the study of biology and pharmacology of paraneurones, Trends Pharmacol. Sci. 3 (1982) 389–392.
[33] F.J. Abajo, M.A. Serrano-Castro, B. Garijo, P. Sánchez-Garcia, Catecholamine release evoked by lithium from the perfused adrenal gland of the cat, Br. J. Pharmacol. 91 (1987) 539–546.
[34] F. de Abajo, M.A. Serrano-Castro, P. Sánchez-Garcia, Catecholamine release from adrenal gland evoked by lithium. A consequence of $[Li]_i-[Ca]_o$ counter-transport mechanism? Ann. N. Y. Acad. Sci. 639 (1991) 665–667.
[35] M.T. de la Fuente, R. Maroto, E. Esquerro, P. Sanchez-Garcia, A.G. Garcia, The actions of ouabain and lithium chloride on cytosolic Ca^{2+} in single chromaffin cells, Eur. J. Pharmacol. 306 (1996) 219–226.
[36] B.T. Layden, A.M. Abukhdeir, N. Minadeo, C.P. Fonseca, L. Carroll, M.M.C.A. Castro, C.F.G.C. Geraldes, F.B. Bryant, D. Mota de Freitas, Effects of Li^+ transport and Li^+ immobilisation on Li^+/Mg^{2+} competition in cells, Biochem. Pharmacol. 66 (2003) 1915–1924.
[37] K.W. Brocklehurst, H.B. Pollard, in: K. Siddle, J. Hutton (Eds.), Peptide Hormones: A Practical Approach, IRL Press, Oxford, 1990, pp. 233–255.
[38] M.K. Patterson Jr., Measurement of growth and viability of cells in culture, Methods Enzymol. 58 (1979) 141–152.
[39] L.W. Role, R.L. Perlman, Purification of adrenal medullary chromaffin cells by density gradient centrifugation, J. Neurosci. Methods 2 (1980) 253–265.
[40] S.P. Wilson, Purification of adrenal chromaffin cells on Renografin gradients, J. Neurosci. Methods 19 (1987) 163–171.
[41] T. Günther, Functional compartmentation of intracellular magnesium, Magnesium 5 (1986) 53–59.
[42] E. Murphy, C.C. Freudenrich, L.A. Levy, R.E. London, M. Lieberman, Monitoring cytosolic free magnesium in cultured chicken heart cells by use of the fluorescent indicator Furaptra, Proc. Natl. Acad. Sci. U. S. A. 86 (1989) 2981–2984.
[43] B. Raju, E. Murphy, L.A. Levy, R.D. Hall, R.E. London, A fluorescent indicator for measuring cytosolic free magnesium, Am. J. Physiol. 256 (1989) C540–C548.
[44] J. Nikolakopoulos, C. Zachariah, D. Mota de Freitas, C.F.G.C. Geraldes, Comparison of the use of gel threads and microcarrier beads in Li^+ transport studies of human neuroblastoma SH-SY5Y cells, Inorg. Chim. Acta 251 (1996) 201–205.
[45] G.R. Painter, E.J. Diliberto Jr., J. Knoth, ^{31}P nuclear magnetic resonance study of the metabolic pools of adenosine triphosphate in cultured bovine adrenal medullary chromaffin cells, Proc. Natl. Acad. Sci. U. S. A. 86 (1989) 2239–2242.
[46] B.E. Ehrlich, J.M. Diamond, Lithium, membranes and manic depressive illness, J. Membr. Biol. 52 (1980) 187–200.
[47] L.-S. Kao, N.S. Cheung, Mechanism of calcium transport across the plasma membrane of bovine chromaffin cells, J. Neurochem. 54 (1990) 1972–1979.
[48] D.A. Powis, K.J. O'Brien, H.R.K. Grafenstein, Calcium export by sodium-calcium exchange in bovine chromaffin cells, Cell Calcium 12 (1991) 493–504.
[49] E. Deval, C. Cognard, Na^+/Ca^{2+} exchange activity in rat skeletal myotubes: effect of lithium ions, Cell Calcium 31 (2002) 37–44.
[50] J. Duhm, Pathways of lithium transport across the human erythrocyte membrane, in: M. Thellier, J.C. Wissocq (Eds.), Lithium Kinetics, Marius, Lancashire, 1992, pp. 27–53.
[51] T.E. DeCoursey, K.G. Chandy, S. Gupta, M.D. Cahalan, Voltage-dependent ion channels in T-lymphocytes, J. Neuroimmunol. 10 (1985) 71–95.
[52] B. Hille, Ionic channels in nerve membranes, Prog. Biophys. Mol. Biol. 21 (1970) 1–32.
[53] J.E. Friedman, P.I. Lelkes, E. Lavie, K. Rosenheck, F. Schneeweiss, A.S. Schneider, Membrane potential and catecholamine secretion by

bovine adrenal chromaffin cells: use of tetraphenylphosphonium distribution and carbocyanine dye fluorescence, J. Neurochem. 44 (1985) 1391–1402.
[54] S. Kitayama, H. Ohtsuki, K. Morita, T. Dohi, A. Tsujimoto, Bis-oxonol experiment on plasma membrane potentials of bovine adrenal chromaffin cells: depolarising stimuli and their possible interaction, Neurosci. Lett. 116 (1990) 275–279.
[55] S. Johansson, Graded action potentials generated by differentiated human neuroblastoma cells, Acta Physiol. Scand. 151 (1994) 331–341.
[56] G.Q. Fox, A morphometric analysis of exocytosis in KCl-stimulated bovine chromaffin cells, Cell Tissue Res. 284 (1996) 303–316.
[57] J.H. Philips, Dynamic aspects of chromaffin granule structure, Neuroscience 7 (1982) 1595–1609.
[58] O. Kaplan, P. Aebersold, J.S. Cohen, Metabolism of peripheral lymphocytes, interleukin-2-activated lymphocytes and tumor-infiltrating lymphocytes from ^{31}P NMR studies, FEBS Lett. 258 (1989) 55–58.
[59] D. Njus, P.A. Sehr, G.K. Radda, G.A. Ritchie, P.J. Seeley, Phosphorous-31 nuclear magnetic resonance studies of active proton translocation in chromaffin granules, Biochemistry 17 (1978) 4337–4343.
[60] R.W. Holz, R.A. Senter, R.R. Sharp, Evidence that the H^+ electrochemical gradient across membranes of chromaffin granules is not involved in exocytosis, J. Biol. Chem. 258 (1983) 7506–7513.
[61] R.P. Casey, D. Njus, G.K. Radda, P.A. Sehr, Active proton uptake by chromaffin granules: observation by amine distribution and phosphorus-31 nuclear magnetic resonance techniques, Biochemistry 16 (1977) 972–977.
[62] R.K. Gupta, J.L. Benovic, Z.B. Rose, The determination of the free magnesium level in the human red blood cell by ^{31}P NMR, J. Biol. Chem. 253 (1978) 6172–6176.
[63] L.P. Montezinho, C.P. Fonseca, C.F.G.C. Geraldes, M.M.C.A. Castro, Quantification and localization of intracellular free Mg^{2+} in bovine chromaffin cells, Metal Based Drugs 9 (2002) 69–80.